Structural And Optical Properties of Tio$_2$/PVA Nanocomposites

M. M. El-Desoky [a,] ,I.M. Morad[a], M.H.Wasfy[a], A.F. Mansour[b],

[a.] *Department of Physics, Faculty of Science, Suez University, Suez, Egypt.*
[b.] *Department of Physics, Faculty of Science, Zagazig University, Zagazig, Egypt.*

Abstract: *The effect of TiO$_2$ nanoparticles doped in PVA on the structural and optical properties of composite films is studied experimentally. Different composite TiO$_2$/PVA films were prepared using solution casting method according to the formula with compositions (wt. %): 0%, 1.33%, 2.6%, 3.9% and 6.6%), and characterized by X-ray diffraction (XRD) and Scanning electron microscope (SEM).The XRD reveals the presence of both anatase and rutile TiO$_2$phases. The average grain size(D) of anatase and rutile TiO$_2$ were found to 63 nm and 27 nm, respectively. The TiO$_2$ nanoparticles formed were highly agglomerated and the average crystal size estimated by micrograph is in range of 21-32 nm which is in closed agreements with the crystal size estimated by Scherer,s. The optical properties of TiO$_2$/ PVA composite films have been investigated. The direct optical band gap is red shifted from 3.87 eV to 2.68 eV with the increase of TiO$_2$content. Dispersion of refractive index (n) has been analyzed using the Wemple–Didomenico single oscillator model and the dispersion parameters (E$_o$, E$_d$) have been determined.*

Keywords: *PVA; Titanium Oxide; Nano-composite; XRD; SEM; optical properties.*

I. Introduction

In the recent years, scaling optical and electronic properties of nanomaterials, which become strongly size dependent focused attention on the preparation of nanoparticle semiconductors[1].TiO$_2$ is the promising material as semiconductor having high photochemical stability and low cost. Well-dispersed Titania nanoparticles with very fine sizes are promising in many applications such as pigments, adsorbents and catalytic supports [2].In almost all of these cases, when the particle size is reduced greatly, especially to several nanometer scales, due to the large surface-to-volume ratio, some novel optical properties can be expected [3].It is not surprising; therefore, that much research has been focused upon the reduction of particle size. Polyvinyl alcohol (PVA) is a polymer with many interesting physical properties attracted researchers due to its attractive film forming, physical properties, good processability, biocompatibility and good chemical resistance. Also, it has excellent as a plasticizer, then reduce its tensile strength. To further enhance the properties of this polymer, the addition of an inorganic material such as TiO$_2$is advantageous for forming a Nano composite; this could be lightweight, flexible and exhibit good mold ability. TiO$_2$ nanoparticle is a high band gap semiconductor that has excellent optical transmittance, high refractive index and good dielectric properties. New technologies are demanding materials with improved structural, electrical and optical properties of traditional PVA films by incorporation of good inorganic materials like TiO$_2$ nanoparticles for the development of new nano devices [5, 6].

In the present work TiO$_2$ nanoparticles have been synthesized using sol gel method and TiO$_2$/ PVA composite films with different concentrations of TiO$_2$ nanomaterials. All samples were characterized by XRD, SEM and UV– visible spectroscopy. Also, we have studied the optical properties of TiO$_2$/ PVA composite films based on TiO$_2$as a filler material and PVA as the main matrix.

II. Experimental

2.1. Materials

Polyvinyl alcohol (PVA) from Sigma Aldrich, with average molecular weight of 50.000 – 85.000 and 97% hydrolyzed was used without further purification. Titanium isopropoxide also were purchased from Aldrich. Reactant solutions were made in doubly distilled water.

2.2. Synthesis of TiO$_2$nanoparticle using Sol-gel technique:

TiO$_2$ was synthesized using a sol-gel method in which the hydrolysis and condensation of titanium alcoxides (titanium isopropoxide (IV)) in aqueous media under acidic conditions. The procedure used is as follows: Solution A:15 ml of titanium isopropoxide added to 45 ml of absolute ethanolat volume ratio (1:3) under continuous stirring for 30 minute until a homogenous white yellow solution produce

---

Solution B:15 ml of H_2O added to 60 ml of absolute ethanol at volume (1:4), HNO_3 was added drop wise until adjacent of the solution PH to be one "acidic solution" and for restrain the hydrolysis process of the solution. The gel preparation process started when both solutions A&B were mixed together and aged under vigorous stirring for 2 h. The gel dries at 80°C in water path for 1 h until most ethanol evaporate after that dries the produced mixture overnight at an oven at 80°C , then the dry gel was calcinated at 500°C for 5hrs were subsequently carried out to obtain desired TiO_2nano-crystalline. These reactions can be schematically represented as follows:

Ti $(OC_3H_7)_4$+ $4H_2O$→ 2Ti $(OH)_4$+ $4C_3H_7OH$(hydrolysis), (I)

Ti $(OH)_4$→ TiO_2xH_2O + (2− x) H_2O(condensation), (II) [7].
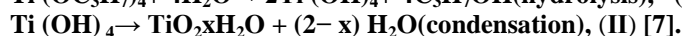
2.3. Preparation of TiO₂ / PVA films

An organic material, Poly Vinyl alcohol (PVA), was selected to be the matrix material in which nanoparticles of TiO_2 were embedded to form the nanocomposites, such organic matrix material is characterized by having high solubility of organic fluorophores, ability to develop film and plate concentrators with good spectral characteristics.

PVA films doped with TiO_2were prepared by solution casting method; the typical procedure for the preparation of TiO_2/PVA nanocomposites is reported as follows:
7.5 gm. of PVA were dissolved in 85ml of distilled water under stirring at 70° C for 2h in order to obtain pure and homogenous solution. At the same time , 0.02 gram , 0.04 gram, 0.06 gram and 0.1 gram was dissolved in 5ml of distilled water for each concentration under stirring at 70°C for 2 hours until make sure that homogeneous solution was obtained , after that the 7.5 gram of PVA solution was added to TiO_2 solution each concentration 1.5 gram under stirring at 70° C for 4 hours until a homogeneous solution , Each solution was placed in a Petri dish and then left in a dust free chamber to dry to remove any residual solvent slowly in air at room temperature for four days to make cast films with different proportions of TiO_2. The weight percent of TiO_2 to PVA are (0, 1.3, 2.6, 3.9 and 6.6) %, the average thickness of these films was found to be in the range of (0.2– 0.3) mm.

2. 4. Characterization

The X-ray diffraction (XRD) patterns of the pure PVA film, TiO_2 powder and the polymer composite films were recorded at room temperature using an X-ray powder diffract meter (Shimadzu XRD 6000) equipped with Cu Kα as radiation source (λ = 1.54Å.)in the 2θ (Bragg angles) range($10^O \leq 2\theta \leq 80^O$) to report the information about their structure. In addition, the surface morphology of these nanocomposites was also examined using scanning electron microscope, SEM (Model Quanta 250 FEG).The particle size and TiO_2nanoparticles morphology were investigated by TEM. The absorbance spectra (A) and the transmittance spectra (T) of the films were recorded at 200–1100 nm wavelength using a dual beam (UVS-2800) UV–Visible spectrophotometer.

III. RESULTS AND DISCUSSION

3.1. X-Ray diffraction analysis

Fig. 1 shows the X-ray diffractograms of the as prepared powder of TiO_2 Nano particles. It shows that XRD patterns exhibited strong diffraction peaks of TiO_2 anatase phase at 2θ= 25.2 ° (101).On the other hand, diffraction peaks at2θ= 27° (110) indicating TiO_2 in the rutile phase. All peaks are in good agreement with the standard spectrum(JCPDS NO.: 88-1175 and 84-1286). The mean grain size (D) of the samples under study can be calculated by Scherrer equation [8]

$$D = \frac{k\lambda}{\beta \cos \theta} \quad (1)$$

Where k ~ 1, λ=0.15406 nm is the wavelength of Cu(Kα) radiation, θ is the Bragg angle of the X-ray diffraction peak and β represents the corrected experimental full-width at half-maximum of the diffraction peak in units of radians. The mean grain sizes of rutile and anatase TiO_2 are 63 nm and 27 nm, respectively. The content of anatase and rutile of all TiO_2 samples were calculated using the following Eq. (2):

$$X_A = 100/ (1+1.265 I_R/I_A) \quad (2)$$

where X_A is the weight fraction of anatase in the mixture, I_A and I_R is intensity of anatase (101) and rutile (110) diffraction, respectively [9]. From XRD data it is found that the anatase to rutile ratio is 68:32 %.Fig.2 shows the X-ray diffraction patterns for pure PVA and PVA/ TiO_2nanocomposites films. It is clear from the figure that there is a broad peak at 2θ ≈ 19.74°corresponding to d spacing of 4.5511Å, and reflection plane (101), and another small peak at 2θ ≈ 29.36° consistent with earlier studies [9], which is attributed to the

polyvinyl alcohol (PVA) indicated the presence of the typical semi-crystalline structure of PVA. However for PVA/ TiO₂, a small diffraction peak is observed at $2\theta \approx 25.3^{\circ}$ corresponding to reflection plane (101) of Anatase TiO₂ and another one at $2\theta \approx 27.3^{\circ}$ corresponding to reflection plane (110) of rutile TiO₂, It is clear that in the lower concentration of TiO₂, the diffraction peaks of TiO₂ is very small compared to that of PVA. These small peaks increase slightly by increasing TiO₂ content reaching 6.6%, as shown in Fig. 2. XRD patterns of PVA/ TiO₂nanocomposites films indicating that there is no chemical interaction between polyvinyl alcohol and the partially- reduced Titanium oxide TiO₂ in forming composite sand TiO₂ has retained its structure even though it is being capped with PVA after formation of composites[10]. Also, the intensity of PVA peak decreases gradually, suggesting a decrease in the degree of crystallinity of PVA. The crystalline nature of PVA results from the strong intermolecular interaction between PVA chains through the intermolecular hydrogen bonding .These interactions between PVAandTiO₂ lead to the decrease of the intermolecular interaction between the PVA chains and thus the crystalline degree [11]. Established a correlation between the intensity of the peak and the degree of crystallinity observed that the intensity of XRD pattern decrease sas the amorphous nature increases with the addition of TiO₂.

3.2. Scanning electron microscope (SEM):
Scanning electron microscope (SEM) was used for the morphological study ofTiO₂nanoparticles, pure PVA and6.6 % TiO₂/PVA nanocomposite film .Fig. 3 (a) shows the SEM images of the as-prepared TiO₂nanoparticles, it is clear thatTiO₂ nanoparticles formed were highly agglomerated and the average crystal size estimated by micrograph is in range of 21-32nm which is in closed agreements with the crystal size estimated by Scherer՜s formula. [12] The spherical shaped particles with clumped distributions are visible through the SEM analysis. The micrograph of pure PVA Fig.3 (b) exhibits a surface without any presence microstructure which is again a characteristic of the amorphous phase.Fig.3(c) shows SEM images of 6.6%(TiO₂/ PVA)nanocomposites film, the images show an increasing amount of TiO₂ in the PVA matrices and also show that TiO₂nanoparticles were uniformly distributed on the PVA film surfaces.

3.4. Optical properties:
3.4.1. The UV-visible absorption spectra
The absorbance spectra of the PVA/TiO₂ nanocomposites films are containing the fundamental peak and the inflection of the PVA and further absorbance band at 335 nm, which corresponding to TiO₂ confirming the formation of the PVA/TiO₂nanocomposites films as shown in fig (4).It is clear that the intensity of the peak increased with increasing TiO₂ concentration because of the absorption of the incident radiation by titanium oxide free electrons. but there is no shift in the peak positions of PVA and TiO₂, indicating that no clear interaction between PVA matrix and TiO₂ nanoparticles i.e. adding different amounts of filler to pure polymer do not change the chemical structure of the material but now physical mixture is formed. Fig.5shows the optical transmittance spectra for TiO₂/PVA films with different TiO₂concentration. It is clear that the transmittance increase with increasing wavelength for different concentration and also decrease with increasing TiO₂ doping concentration this is due to the fact that , TiO₂ particles absorb and scatter the incident light from PVA film .

The real dielectric depends on n^2 and K^2, but the imaginary dielectric depends on k and n. The real and imaginary dielectric constant (ε_1 and ε_2) have been calculated from Equations (3, 4), the values of the real dielectric constant are high with respect to the imaginary dielectric constant, because they are dependent on n and k values.

$$\varepsilon_r \ = \ n^2 - k^2, \qquad (3)$$

$$\varepsilon_i \ = \ 2nk. \qquad (4)$$

The extinction coefficient k is responsible for attenuation of light as ε_2 is responsible for attenuation of electrical field, causing dielectric loss. Fig.6 (a) and (b) show the change of these constants with wavelengths for PVA-TiO₂, It was noted that the real and the imaginary parst increase slightly with increasing the TiO₂ concentration . At higher wavelengths the dielectric parameters are almost constant

3.4.2. Determination of optical band gap:
The fundamental absorption, which corresponds to electron excitation from the valence band to the conduction band, can be used to determine the value of the optical band gap (E_g) and it is related to the optical transition. The E_g values can be obtained from the optical absorption spectra by the following relation [14]:

$$\alpha h\nu = B(h\nu - E_{op})^n \quad (5)$$

α is the absorption coefficient, which is calculated using the Beer- Lambert's relation [15]

$$\alpha = 2.303 \frac{A}{t} \qquad (6)$$

A and t are the absorbance and the thickness of the film. B is the parameter that depends on the inter band transition probability, hv is the incident photon energy, E_g is the optical band gap and (n) is an index characterizing the nature of the electronic transitions causing the optical absorption. n can take values 1/2, 3/2, 2, and 3 for direct allowed, direct forbidden, indirect allowed and indirect forbidden transitions, respectively. Fig.7shows the relation between absorption edges (αhv)^2 for pure PVA and TiO₂/ PVA composites as a function of photon energy (hv). At extension of the curve to the value (αhv) ^{2}= 0, we get the direct band gap of the composites. The obtained values of optical band gap of the composites are tabulated in table (1). It is showed that the values of energy gap decrease with increasing TiO₂concentration, this decrease because as TiO₂ content is responsible for the formation of some defects in the films. These defects produce the localized states in the optical band gap and overlap. These overlaps give an evidence for decreasing energy band gap when the TiO₂ content is increased in the polymeric matrix .In other words, the decreased in the optical gap reflects the increase in the degree of disorder in the films.

The absorption coefficient near the fundamental absorption edge is exponentially dependent on the incident photon energy and obeys the empirical Urbach relation [16]

$$\alpha = \alpha_o \exp\left(\frac{E}{E_U}\right) \qquad (7)$$

where E_u is the optical activation energy known as the Urbach energy which represents the band width of the tail of localized states in the band gap, and α_o is constant. The optical activation energy, E_u was determined using the least square fitting and listed in Table 1. Figure 8 shows the plot of (lnα) versus photon energy E (eV) for all samples before and after being doped.Urbach energy values of thefilms increase with increasing titanium oxide content , this increase is attributed to the increase of disorder of the PVA matrix occurred by TiO₂ dopant. Also the increase in TiO₂ concentrations leads to a redistribution of stated from band to tail, thus allows for a greater number of possible band to tail and tail transitions[17]

3.4.3. Determination of optical constants:

The refractive index (n) is a one of the fundamental properties of a material which have a potentially role in mostapplications of the optical devices. One method of calculating the refractive index (n) is by using the reflectance (R) and the extinction coefficient (k) of films [18]:

$$n = \frac{(1+R)}{(1-R)} + \sqrt{\frac{4R}{(R-1)^2} - k^2} \qquad (8)$$

Figure (9) shows the refractive index (n) of pure PVA and TiO₂/ PVA films as a function of wavelength. The refractive index increases with increasing TiO₂concentration; this behavior can be attributed to the increasing of the packing density as a result of filler content. The refraction index decreases at the greatest wavelengths and increases at the greatest doping concentration, because the transmission of the longest wavelength is more. In fact, when the incident light interacts with a material has a large amount of particles, the refraction will be high and hence the refractivity of the films will be increased.

The dispersion of refractive index below the inter-band absorption edge has been analyzed using the single oscillator model developed by Wemple and Didomenico [20].

$$n^2 - 1 = \frac{E_o E_d}{E_o^2 - (hv)^2} \qquad (9)$$

Where, E_o is the oscillator energy (which is a measure of the average excitation energy for electronic transitions), and E_d is the dispersion energy (which is a measure of the average strength of inter-band optical transitions).

Plotting $1/(n^2 - 1)$ versus (hv)^2, as shown in figure (10), the values of E_o and E_d can be obtained from the intercept and slope of the linear fitted lines, respectively. The obtained values of E_o and E_d are tabulated in table (1). It can be discerned from table (1) that values of E_o, decrease with increasing concentration of TiO₂ in PVA matrix. This decrease because of increasing the localized states in the energy gap which in turn enhances the low energy transitions leading to a decrease in the value of E_o. The dispersion energy E_d, is associated with changes in the structural order of the material [21], which explain the increase in E_d values with increasing TiO₂ concentration. The oscillator energy E_o is varies in proportion empirically to the Tauc gap, E_g^{opt}, and for our TiO₂/ PVA composites is $E_o=1.9E_g$. by comparison with the value of the optical energy gap has been tabulated

in Table (1). It seems to be in good agreement with the data obtained from E$_o$. The static refractive index n$_o$, at zero photon energy and then the static dielectric constant $\varepsilon_s = n_o^2$, are also evaluated and tabulated in table (1). The static refractive index and the static dielectric constant of TiO$_2$/ PVA composites increase with increasing TiO$_2$ concentration.

The average inter-band oscillator wavelength λ_o and the average oscillator strength S$_o$ for TiO$_2$/ PVA nanocomposite films, can be obtained using the single term Sellmeir oscillator as follows [19]:

$$\frac{n_\infty^2 - 1}{n^2 - 1} = 1 - (\frac{\lambda_o}{\lambda})^2 \qquad (10)$$

By plotting the relation between $1/(n^2 - 1)$ and $(1/\lambda^2)$ for the pure PVA and TiO$_2$/ PVA composites as shown in figure (11), values of λ_o and S$_o$ can be obtained and tabulated in table (2). It is noticed that S$_o$ and λ_o are increase with increasing TiO$_2$ concentration.

The obtained data of refractive index n can be further analyzed to obtain the high frequency dielectric constant ε_∞ according to the following procedure. According to El-Desoky [22] the real part of the dielectric constant is given by:

$$\varepsilon' = n^2 - k^2 = \varepsilon_\infty - \frac{e^2 N}{\pi \varepsilon_o m^* c^2} \lambda^2 \qquad (11)$$

Where ε_∞ is the high-frequency dielectric constant λ is the wavelength, e is the charge of the electron, N is the free charge-carrier concentration, ε_o is the permittivity of the free space, m* the effective mass of the charge carriers in units of kg, and c is the velocity of light. By plotting the relation between ε' and λ^2, as shown in figure (12) we can calculate ε_∞ and (N/m*) from the intercept and the slope of the linear portion of that curve, respectively. Also, the long wavelength refractive index n$_\infty$, is calculated using the relation $\varepsilon_\infty = n_\infty^2$. It is noticed that free carriers increase (N/m*) of the TiO$_2$/ PVA composites with increasing TiO$_2$ content as shown in table (2). Furthermore, ε_∞ and n$_\infty$ are increased with increasing TiO$_2$ content.

According to these results the optical constants of these films could be controlled by TiO$_2$ content. The quantitative measurements of these parameters may help in tailoring and modeling the properties of such films for their use in optical and optoelectronic components and devices.

The optical conductivity σ_{op} is related to refractive index (n), light speed (c) and absorption coefficient (α) can be obtained by the following equation [23]:

$$\sigma_{op} = \frac{nc\alpha}{4\pi} \qquad (12)$$

The term "optical conductivity" means the electrical conductivity results from the movement of the charge carriers due to alternating electric field of the incident electromagnetic waves. Figure (13) show the optical conductivity of pure PVA and TiO$_2$/ PVA composite films. It is noticed that the optical conductivity increases with increasing TiO$_2$ content. This increase because of creation of new levels in the band gap, lead to facilitate the crossing of electrons from the valence band to these local levels to the conduction band, consequently the band gap decreases and the conductivity increase.

IV. Conclusions

Titanium oxide was prepared by sol gel method. The composite films TiO$_2$/PVA were prepared by the well-known solution casting technique. X-ray diffraction (XRD) was confirmed the formation of the two phases in all composites. TiO$_2$ nano-powder enhanced the optical properties of the PVA matrix. The composite with concentration (6.6% w.t) is the characteristic one, where have the highest absorption, lowest energy gap and the highest optical conductivity. These entire advantages make the TiO$_2$/ PVA composite with the concentration 6.6% wt. has wide range for solar cell applications, especially for solar cells photoelectrode

References

[1]. M.Tomkiiewicz, Catal. Today 58 (2000) 115.
[2]. G.Ramakrishna, H.N. Ghosh, Langmuir 19 (2003) 505.
[3]. S.Sahni, S.B.Reddy, B.S.Murty, Materials Science and Engineering A 452-453 (2007) 758.
[4]. J. Fromageau,E. Brusseau, D. Vray , G. Gimenez , P. Delachartre, 2003. Characterization of PVA cryogel for intravascular ultrasound elasticity imaging. IEEE Transactions on Ultrasonic, 50(10):1318-1324.
[5]. M. Kokabi, M. Sirousazar, Z. Hassan, Eur. Polym. J. 43 (2007) 773.
[6]. D. Vorkapic and T. Matsoukas, J. Amer. Ceram.Soc. 81(1998)2815.

[7].   B. Pejova, I. Grozdanov, Three dimensional confinement effects in semicoduct-ing zinc selenide quantum dots deposited in thin film form, Mater. Chem. Phys. 90 (2005) 35.
[8].   D. Mardare, M.T asca, M. Delibas and G.I. Rusu, Appl.Surf.Sci., 156 (2000) 200.
[9].   Praveen C. Ramamurthy, Aashis S. Roy, Satyajit Gupta, S. Sindhu, Ameena Parveen, Part B 47 (2013) 314.
[10].   R.M. Hodge, G.H. Edwrd, E.P. Simon, Polymer 37 (1966) 1371.
[11].   M.Vishwas,K.NarasimhaRao,D.Neelapriya,AshokM.Raichure,R.P.S.Chakradhar,K.Venkateswarlu, Procedia Materials Science 5 (2014) 847.
[12].   O. G. Abdullah and D. R. Saber, Applied Mechanics and Materials, 110–116 (2012)177.
[13].   R. Seoudi, A.B. El-bially, W. Eisa, A. A. Shabaka, S. I. soliman, R. K. Abd El-Hamid,   R. A. Ramadan, Journal of Applied Science Research 8 (2) (2012) 658.
[14].   P.P.R. Sahay, K. Nath, S. Tewari, Cryst. Res. Technol. 42 (2007) 275.
[15].   F. Urbach, The long wavelength edge of photographic sensitivity of the electron absorption of solids, Phys. Rev. 92 (1953) 1324.
[16].   ] S.K. O'Leary, S. Zukotynski, J.M. Perz, Disorder and optical absorption in amorphous silicon and amorphous germanium, J. Non-Crystalline Solids 210(1997)249.
[17].   I.S. Yahia, A. A. M. Farag, M. Cavas, F. Yakuphanoglu, Superlattice. Microst. 53 (2013) 63.
[18].   H.M. Zidan, A. El-Khodary, I.A. El-sayed, H.I. El-Bohy, J. Appl. Polym. Sci. 117 (2010) 1416.
[19].   S. H. Wemple and M. Jr. Didomenico, Phys. Rev. B 3, (1971) 1338.
[20].   S. H. Shaaker, W. A. Hussain, H. A. Badran, Advances in Applied Science Research, 3 (5) (2012) 2940.
[21].   M.M. El-Desoky , M.S. Al-Assiri, A. Alyamani, A. Al-Hajry, A. Al-Mogeeth, A.A. Bahgat, Optics & Laser Technology 42 (2010) 994.
[22].   R. Das, and S. Pandey, "Comparison of optical properties of bulk and nano crystalline thin films of CdS using different precursors", International Journal of Material Science 1(1), (2011)35.
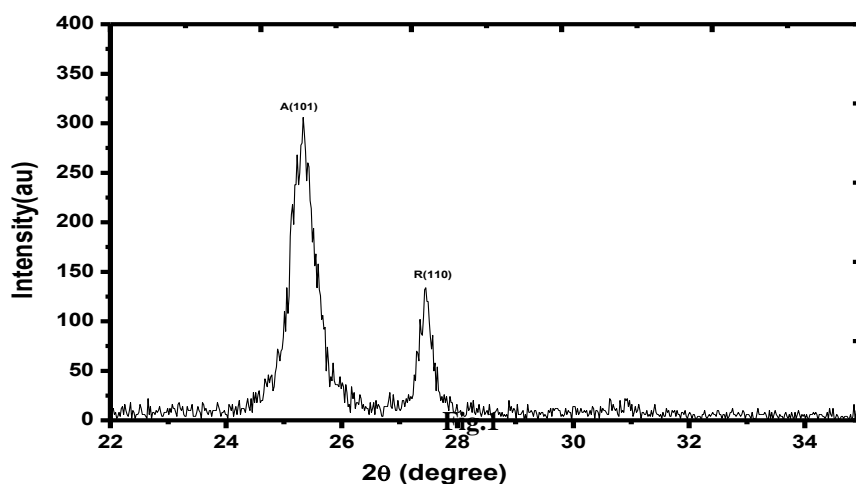
Fig. 1
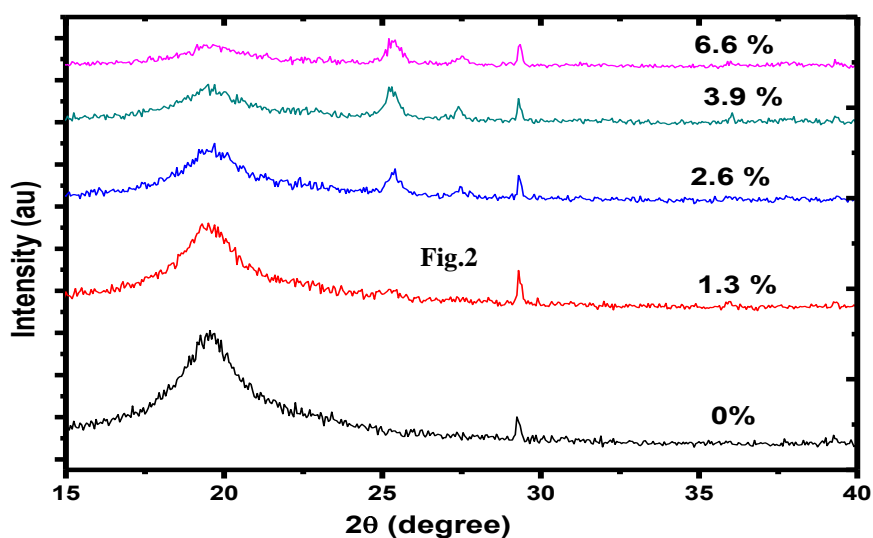
Fig. 2
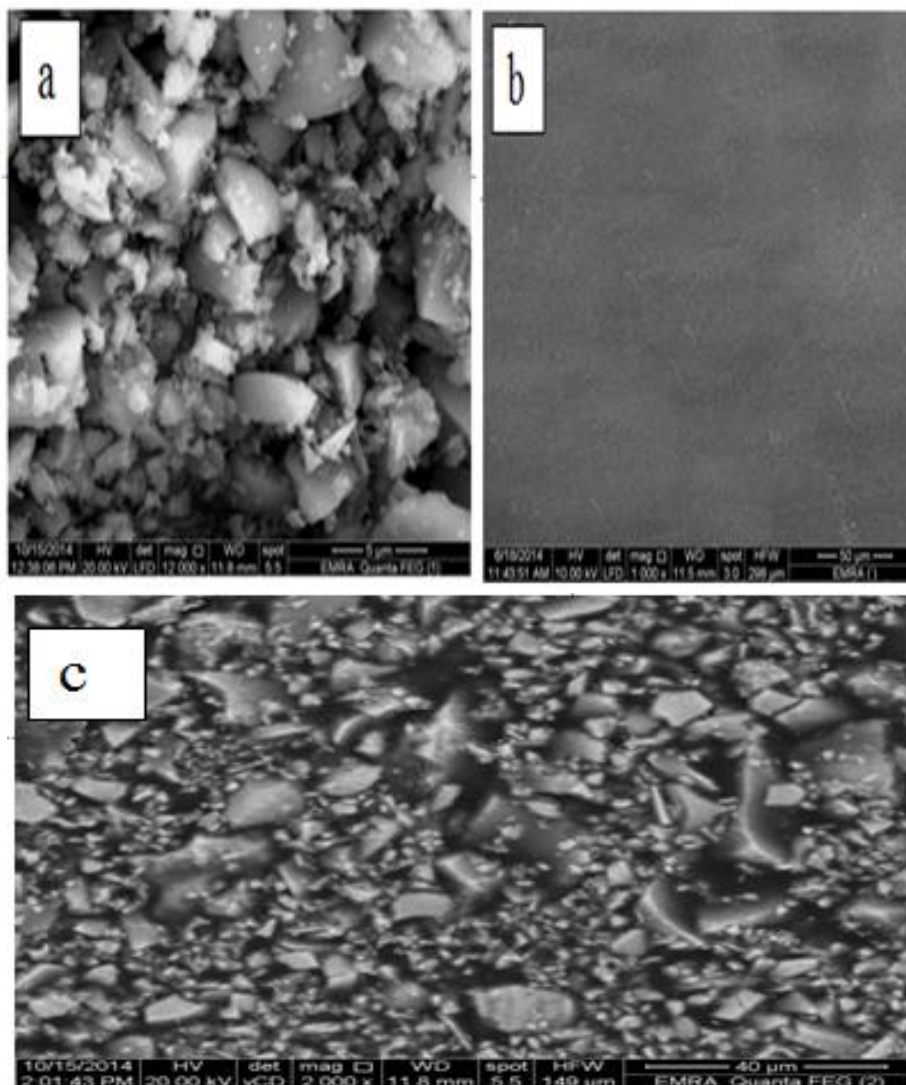
Fig. 3
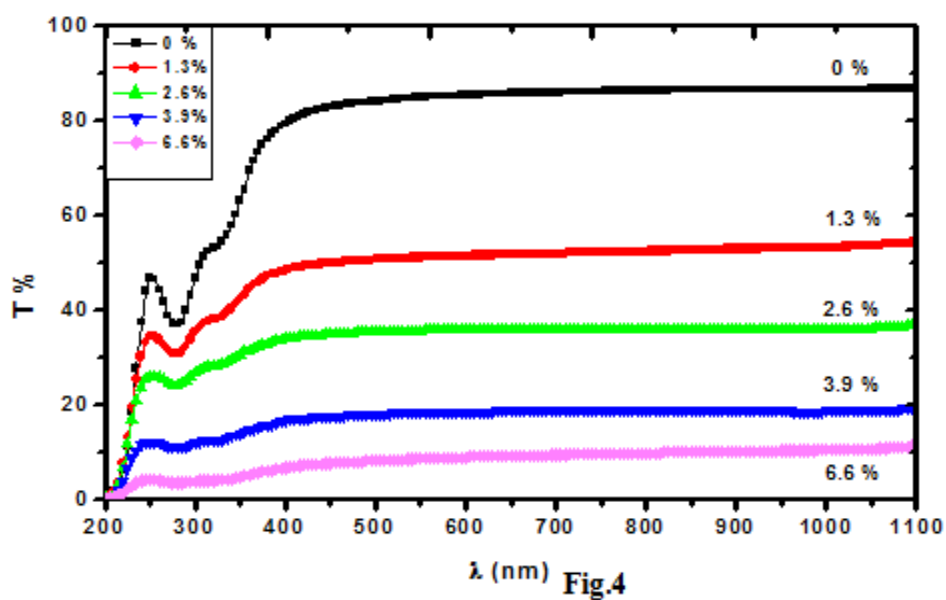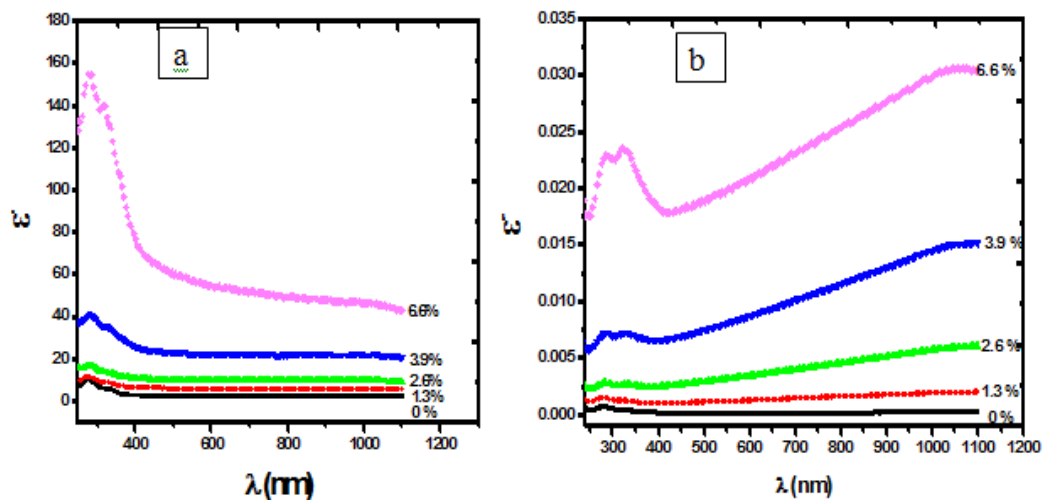
Fig.5
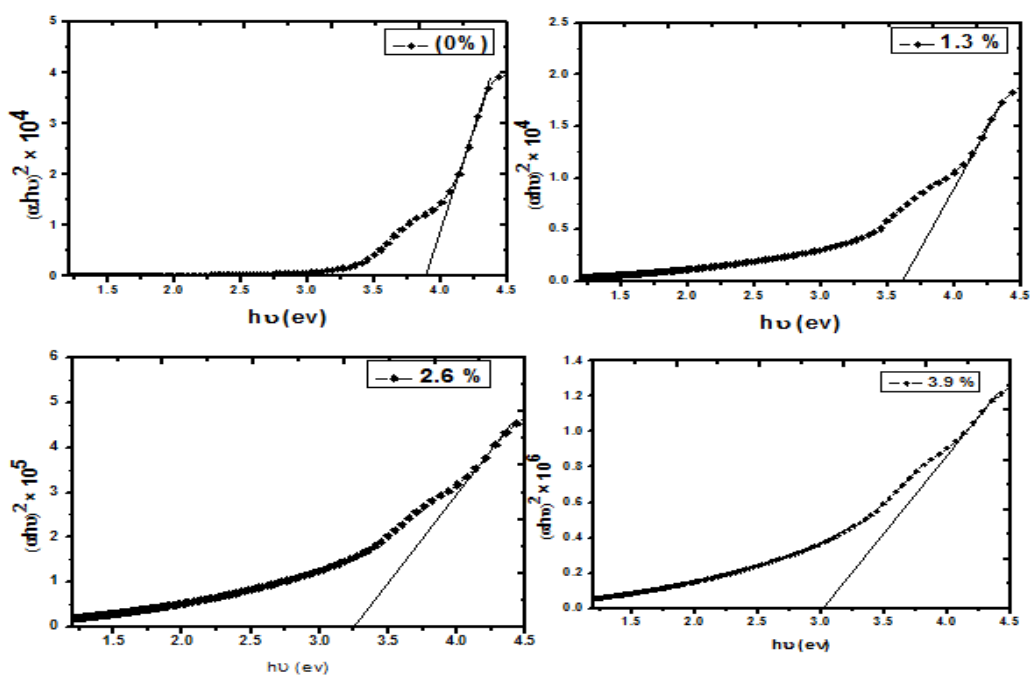
Fig. 6
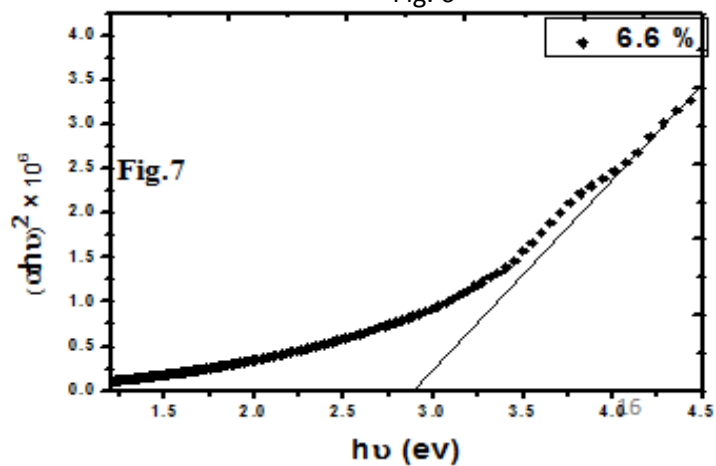
Fig.7
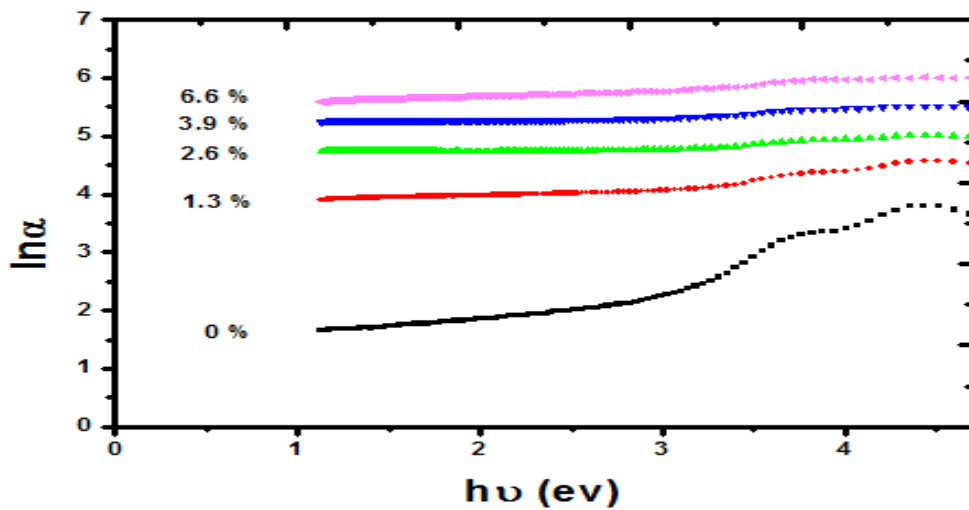
Fig.8
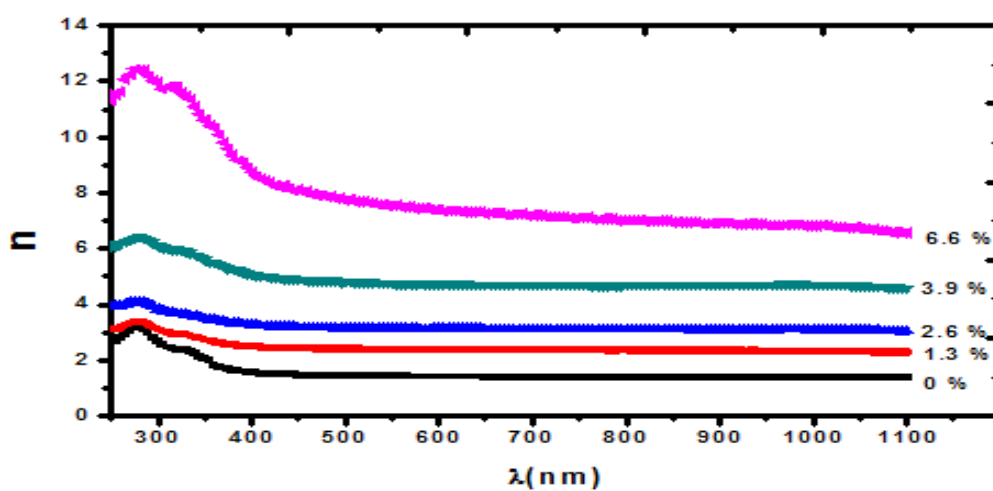
Fig.9
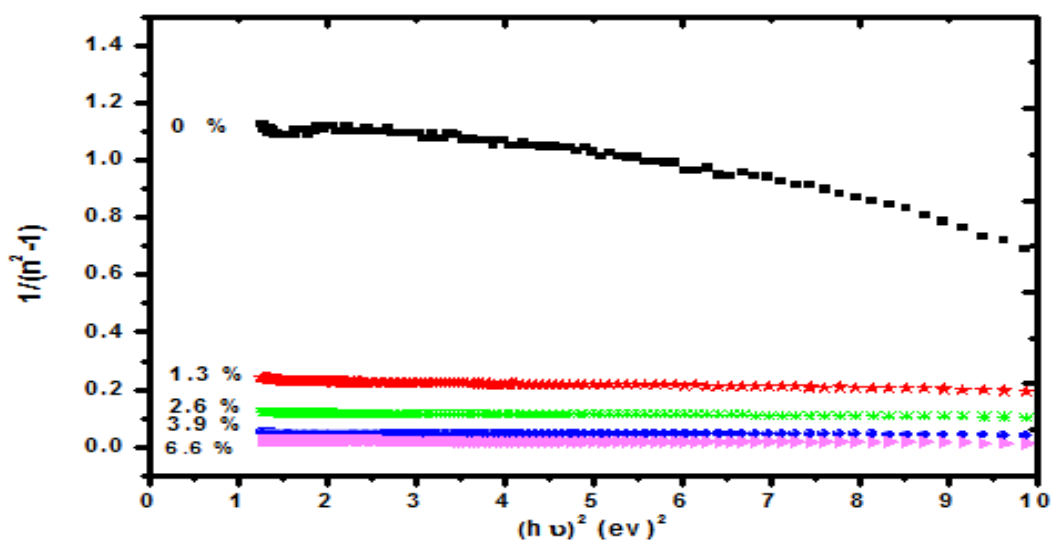
Fig.10
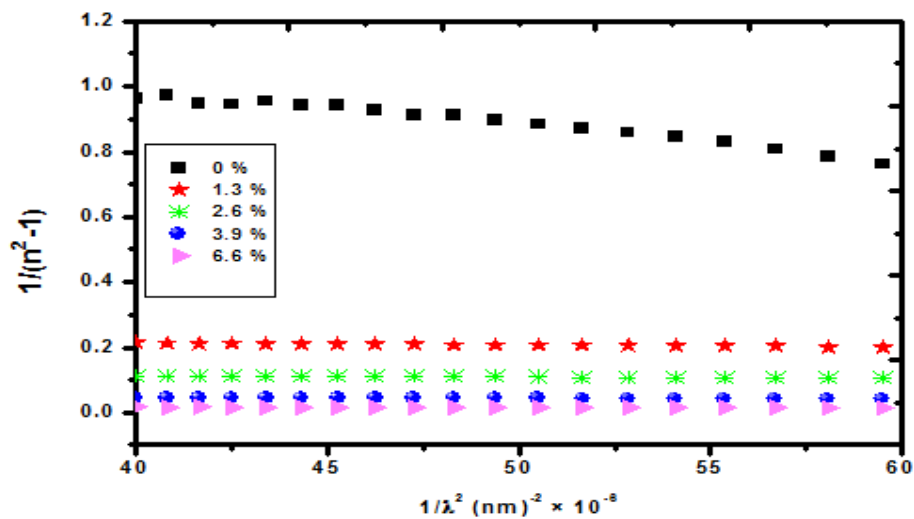
Fig.11
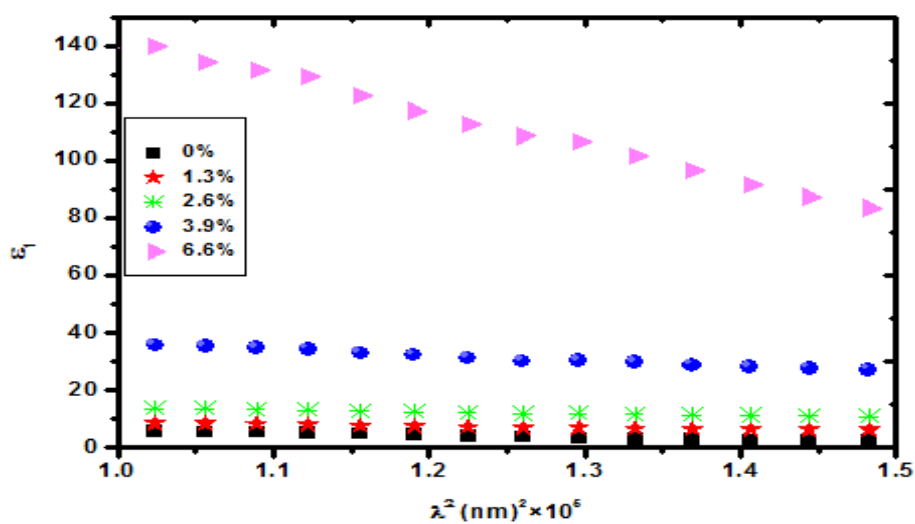
Fig.12
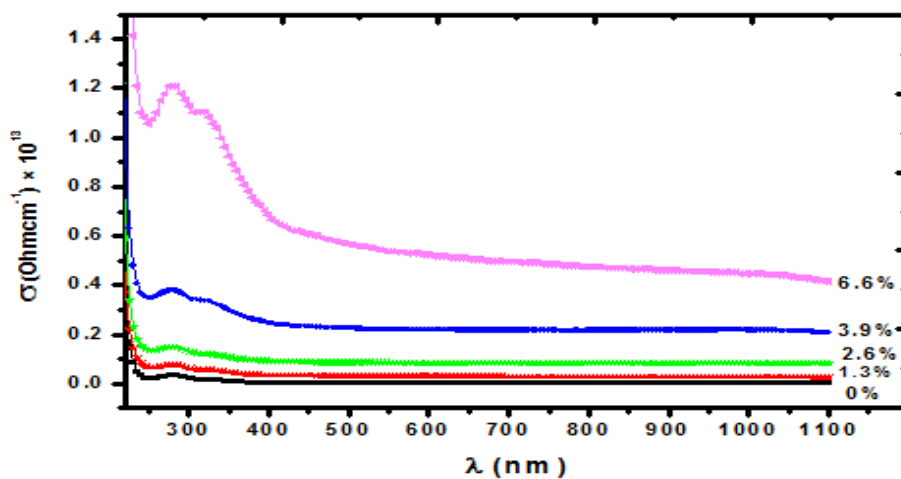
Fig.13

Table (1): The optical parameters of Titanium oxide (TiO$_2$) doped PVA.

TiO$_2$ %	$E_g^{Optical}$ (ev)	E_g^W (ev)	E$_o$(ev)	E$_u$ (ev)	E$_d$ (eV)	n$_o$	ε$_s$	λo (nm)
0	3.87	3.890	7.39	0.587	4.52	1.27	5.483	226.402
1.3	3.62	3.731	7.08	0.707	35.44	2.45	8.570	131.608
2.6	3.3	3.343	6.35	0.727	52.49	3.04	9.431	144.831
3.9	3.1	2.632	5.00	0.954	100	4.58	7.301	170.003
6.6	2.79	2.515	4.78	1.733	207.11	6.66	4.934	251.577

Table (2): Other optical parameters of Titanium oxide (TiO$_2$) doped PVA.

TiO$_2$ %	S$_0$ *10^{13}(m^{-2})	λo (nm)	N/m*(m^{-3})*10^{56}	n$_\infty$	ε$_\infty$ = n^2
0	1.59	226.402	7.39	1.899	3.60484
1.3	20.49	131.608	7.99	2.721	7.40604
2.6	48.32	144.831	13.09	3.582	12.82897
3.9	68.01	170.003	50.81	5.841	34.12096
6.6	69.91	251.577	42.83	12.138	147.3424

(Figure captions)

Fig 1: XRD pattern for TiO$_2$ nanoparticles
Fig 2: XRD pattern for TiO$_2$/PVA nanocomposites
Fig.3: SEM images of (a) TiO$_2$ nanoparticles (b) Pure PVA film (c) TiO$_2$/PVA nano-composites
Fig.4: UV-visible absorption spectra of PVA/TiO$_2$ nanocomposite films.
Fig 5: Transmittance spectra as a function of wavelength for PVA/TiO$_2$ nanocomposite films.
Fig 6: (a) Real part and (b) Imaginary part of dielectric constant as a function of wavelength for TiO$_2$/PVA nanocomposite films
Fig. 7: Relation between (αhv)^2 and (hv) for pure PVA and TiO$_2$/ PVA composites
Fig 8: Variation of the Urbach plot of ln α as a function of photon energy (hv) for PVA/TiO$_2$ nanocomposites films.
Fig 9: Refractive index (n) as a function of wavelength for PVA/TiO$_2$ nanocomposites films.
Fig 10: Relation between 1/ n^2- 1 and hv^2 for PVA/TiO$_2$ nanocomposites films.
Fig 11: Relation between 1/ n^2- 1 and 1/λ^2 for PVA/TiO$_2$ nanocomposites films.
Fig 12: plot of ε$_1$ as a function of λ^2 for PVA/TiO$_2$ nanocomposites films.
Fig 13: The optical conductivity as a function of wavelength for TiO$_2$/ PVA nanocomposite films.